

# Gas Leaks through Corrosion Defects of Buried Gas Transmission Pipelines

CRISTIAN EPARU<sup>1\*</sup>, MIHAI ALBULESCU<sup>1\*</sup>, SORIN NEACSU<sup>1</sup>, CATALIN ALBULESCU<sup>2</sup>

<sup>1</sup> Petroleum - Gas University of Ploiesti, 39 Bucuresti Blvd., 100520, Ploiesti, Romania

<sup>2</sup> SNGN ROMGAZ SA-Ploiesti Branch, 184 Gr. Cantacuzino, 100507, Ploiesti, Romania

*Taking as a starting point the appearance of corrosion flaws along the natural gas pipelines in Romania, this paper presents an analysis undertaken using the numerical simulation of gas leakage through defects of buried pipelines. In order to assess and analyze the effect of such failures an original 3D numerical model was designed. Simulations have been carried out considering different burial depths and different positions of defects on a pressurized pipeline.*

*Keywords: leakage, gas, failure/defect, corrosion*

As it affects both the natural gas balance and the safety of the operation itself an important issue which needs to be considered when discussing the operation of gas transport systems is the gas leakage through various defects. These defects may occur accidentally or may be caused by corrosion [1]. Corrosion defects are usually minor. These can be detected indirectly by the effects they produce, namely by gas leaks [2]. According to Stan and Popoviciu [3], if such failures occur in a densely populated area the resulting gas leakages may have dramatic consequences.

This paper presents an analysis of gas leaks through holes caused by corrosion defects in the case of buried natural gas transmission pipelines, which feature a high-pressure level (20-40bar). The phenomenon is a complex one due to the position of the pipe, which is buried at a depth of 1m, the gases diffused by fault seep into the ground and some of them reach the ground surface where, in contact with the air, they can lead to dangerous accumulations in the atmosphere [4].

The analysis was performed with the help of an original 3D numerical model that allowed the simulation of several types of failure situations, featuring various defects in different positions, different burial depths, multiple defects, etc.

The gas leak flows emerging from the soil caused by the gas leakage through defects as well as their diffusion through the soil in the vicinity of the pipeline were carefully assessed for all the situations considered. Simultaneously, the area affected by gas leaks was also assessed.

In order to design the numerical model a steel gas pipeline with a diameter of 20 "(488.95mm) has been selected. Through this pipeline the natural gas is transported at a 40 bar pressure and along it there have been developed small-sized defects (diameter 4 mm).

In order to determine the gas leak flows through a buried pipeline the soil in its vicinity has been shaped by creating a rectangular network in which the gas flow equations have been defined by means of finite differences so that to determine the pressure field generated by the failure which causes the gas seep through the soil.

## Presentation of the numerical model

In the case of buried transmission pipelines which have defects, the gas escaping through the defect diffuses

through the soil and then resurfaces. The gas flow rate which is lost through the pipeline depends on the pressure level of the gas in the pipeline, on the surface of the defect and also on the pressure gradient which is established in the vicinity of the pipeline, which in its turn is influenced by the properties of the porous medium [2, 5].

The problem of gas leakage through defects along the buried pipelines is a complex problem which requires a numerical approach.

To study the various aspects of gas leakage through defects along buried pipes a three-dimensional numerical model has been designed, a model which is capable of simulating the unsteady gas movement through the soil around the pipelines by observing the real geometry.

The equations of the model are represented by the equations specific to gas movement through the porous medium [5-7].

$$\frac{\partial}{\partial x} \left( \frac{k}{\mu Z} \frac{\partial p^2}{\partial x} \right) + \frac{\partial}{\partial y} \left( \frac{k}{\mu Z} \frac{\partial p^2}{\partial y} \right) + \frac{\partial}{\partial z} \left( \frac{k}{\mu Z} \frac{\partial p^2}{\partial z} \right) = 2m \frac{\partial}{\partial \tau} \left( \frac{p}{Z} \right) \quad (1)$$

where:

$p$  = pressure of the gas;  
 $x, y, z$  = spatial coordinates;  
 $Z$  = compressibility factor;  
 $m$  = porosity;  
 $\mu$  - dynamic viscosity;  
 $k$  - permeability of the soil.

The geometry of the integration domain and a node in the discrete network are outlined in figure 1. The dimensions are measured in millimetres.

To integrate equation (1) in time and space the volume of the soil around the pipe is divided into elementary volumes. The functions of equation (1), the pressure level, the compression factor and the permeability are defined by the centres of the elementary volumes becoming thus network functions.

The function value within a network node is defined by using node indexes. Example  $p_{i,j,k}$  - represents the pressure in the node  $i, j, k$ . Indices  $i, j, k$  stand for indices corresponding to spatial divisions of the coordinate axes, defined as:  $Ox: i = 1, 2, \dots, Nx$ ;  $Oy: j = 1, 2, \dots, Ny$ ;  $Oz: z = 1, 2, \dots, Nz$ ; the index  $n$  has been used for the temporary division.

Considering any of the network nodes equation (1) develops into finite differences.

\* email: cristian.eparu@gmail.com; Tel.: 0722483680

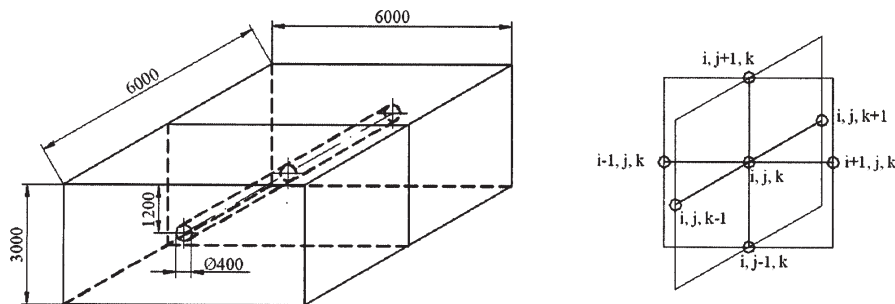


Fig. 1. The geometry of the numerical model and a node in the discrete network

To be able to take into account different permeability areas, the permeability of the medium is considered as being variable. It is defined as a network function in each node. Considering  $T$  - local transmissibility between two adjacent nodes,  $i$  and  $i + 1$ , and the definition is as follows:

$$T_{i+\frac{1}{2},j,k} = \frac{1}{2} \left[ \left( \frac{k}{\mu z} \right)_{i+1,j,k} + \left( \frac{k}{\mu z} \right)_{i,j,k} \right] \quad (2)$$

$$\frac{\partial}{\partial x} \left( \frac{k}{\mu z} \frac{\partial p^2}{\partial x} \right) \approx \frac{1}{\Delta x} \left[ T_{i+\frac{1}{2},j,k} \frac{(p_{i+1,j,k}^n - p_{i,j,k}^n)(p_{i+1,j,k}^{n-1} + p_{i,j,k}^{n-1})}{\Delta x} - T_{i-\frac{1}{2},j,k} \frac{(p_{i,j,k}^n - p_{i-1,j,k}^n)(p_{i,j,k}^{n-1} + p_{i-1,j,k}^{n-1})}{\Delta x} \right] = A \quad (3)$$

Since the equation (1) is non-linear, a method of linearization has been used for  $p^2$ ; this method has been obtained by decomposing the squares difference and by separating the moments of time used to define the variables of the right side:

$$p_{i+1}^2 - p_i^2 = (p_{i+1}^n - p_i^n)(p_{i+1}^{n-1} + p_i^{n-1}) \quad (4)$$

The terms of relationship number 3 were observed at three different time steps using a scheme with 3 time levels:

$n+1$  - variables which are to be calculated at the new time level;

$n$  - variables already calculated for the considered time level;

$n-1$  - variables calculated for the previous step.

By introducing the notations  $A$ ,  $B$  and  $C$ , the transformation of equation (1) in finite differences is performed as such:

$$\frac{\partial}{\partial y} \left( \frac{k}{\mu z} \frac{\partial p^2}{\partial y} \right) \approx \frac{1}{\Delta y} \left[ T_{i,j+\frac{1}{2},k} \frac{(p_{i,j+1,k}^n - p_{i,j,k}^n)(p_{i,j+1,k}^{n-1} + p_{i,j,k}^{n-1})}{\Delta y} - T_{i,j-\frac{1}{2},k} \frac{(p_{i,j,k}^n - p_{i,j-1,k}^n)(p_{i,j,k}^{n-1} + p_{i,j-1,k}^{n-1})}{\Delta y} \right] = B \quad (5)$$

$$\frac{\partial}{\partial z} \left( \frac{k}{\mu z} \frac{\partial p^2}{\partial z} \right) \approx \frac{1}{\Delta z} \left[ T_{i,j,k+\frac{1}{2}} \frac{(p_{i,j,k+1}^n - p_{i,j,k}^n)(p_{i,j,k+1}^{n-1} + p_{i,j,k}^{n-1})}{\Delta z} - T_{i,j,k-\frac{1}{2}} \frac{(p_{i,j,k}^n - p_{i,j,k-1}^n)(p_{i,j,k}^{n-1} + p_{i,j,k-1}^{n-1})}{\Delta z} \right] = C \quad (6)$$

In order to make the term of the right side of equation (1) a discrete one, it is conceived that both the pressure and the compressibility factor are variable depending on the time.

$$2m \frac{\partial}{\partial \tau} \left( \frac{p}{z} \right) = \frac{1}{z} \frac{\partial p}{\partial \tau} + p \frac{\partial}{\partial \tau} \frac{1}{z} \quad (7)$$

The right member of the relation (7) is presented as a time function as follows

$$2m \frac{\partial}{\partial \tau} \left( \frac{p}{z} \right) \approx \frac{2m}{z_{i,j,k}} \frac{p_{i,j,k}^{n+1} - p_{i,j,k}^n}{\Delta \tau} + p_{i,j,k}^n \frac{2m}{\Delta \tau} \left( \frac{1}{z_{i,j,k}^n} - \frac{1}{z_{i,j,k}^{n-1}} \right) \quad (8)$$

Using the notations of the equations (3), (5) and (6) we obtain the calculation formula for the pressure in the node  $i, j, k$  at the new time point  $n + 1$ :

$$p_{i,j,k}^{n+1} = p_{i,j,k}^n - z_{i,j,k}^n \cdot p_{i,j,k}^n \left( \frac{1}{z_{i,j,k}^n} - \frac{1}{z_{i,j,k}^{n-1}} \right) + \frac{z_{i,j,k}^n}{2m} \Delta \tau \cdot (A + B + C) \quad (9)$$

Relation (9) is valid for all nodes along the network. This generates a linear system of equations having the size of the discrete network which has been solved by means of iterative methods.

In order to integrate the system of equations initial and boundary conditions are required. For the initial conditions, the pressures within the network nodes were considered equal to the hydrostatic pressure at the depth of the node.

The boundary conditions have been established within the nodes of the defect, where the condition was of the Dirichlet type, and the pressure within the nodes of the defect was considered equal to the pressure in the pipe [5, 8]. The conditions set for the domain boundary were of Neumann type, namely perfectly permeable borders.

#### Outlining the results obtained by means of numerical model

All the presented results have been obtained for cases of one or more corrosion defects having a diameter of 4 mm. In all cases the gas pressure in the pipe was of 40 bar.

#### Results specific to transitory regime

The results in this section highlight the duration of the transitory regime and the variation of parameters during this period. As emphasized by Stan [9], this regime begins once the gas starts leaking through the defect and it ends when the leaking parameters stabilize over time.

The results outlined in figure 2 show that the transitory regime is characterized by a short duration. In the case presented, it takes two minutes. After this period it is observed that the leaking parameters stabilize and the leak flow can be considered stationary.

The values of the flow depicted in figure 2 have been obtained by integrating the flow rates proper to the elementary surfaces from the plane of the ground surface above the pipeline. Flow values calculated with the numerical model are represented on the graph by points, while the solid curve represents a function obtained by means of regression and it has the expression:

$$Q = a + bx + \frac{c}{x} \left[ \frac{Nmc}{h} \right] \quad (10)$$

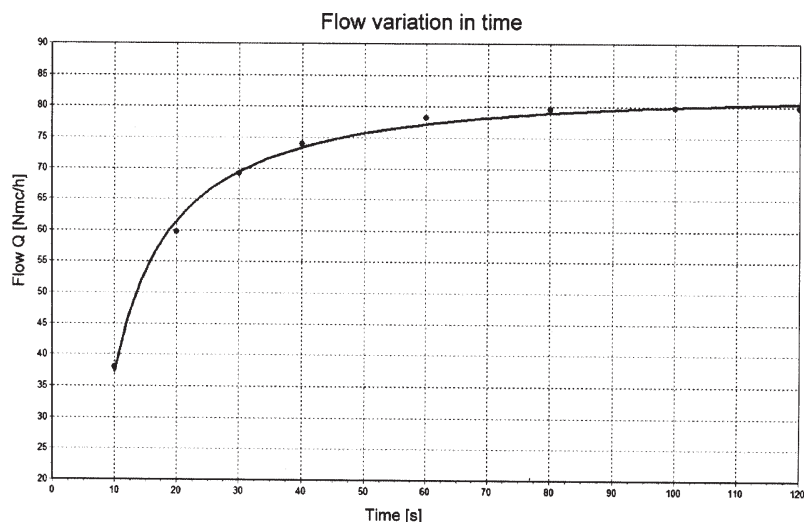


Fig. 2. Variation of gas flow in the transitory period

where:  $x$  - represents time calculated in seconds, and the coefficient values are:  $a = 86.065757$ ,  $b = -0.012724536$ ,  $c = -486.54634$ ;

Figure 3 graphically depicts the distribution of gas flow diffused through the soil, on a horizontal plane, on the surface of the ground above the pipeline, at the end of the transitory period. It is observed that the gas flow leaked through the defect and infiltrated through the soil spreads over a fairly large area. Maximum values are disposed on the defect axis and they decrease as we move away from this axis.

When analyzing the development manner of the area affected by gas leakage in the transitory period it can be observed that the diameter of the area affected by gas seepage increases when the leaking through the defect begins and it reaches a maximum value at the end of the transitory period. The results are graphically outlined in figure 4.

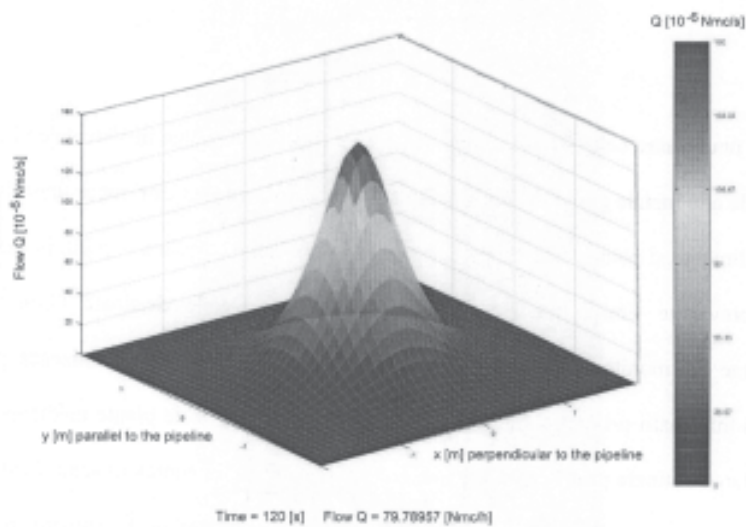


Fig. 3. Distribution of the flow diffused through the soil at 120 s

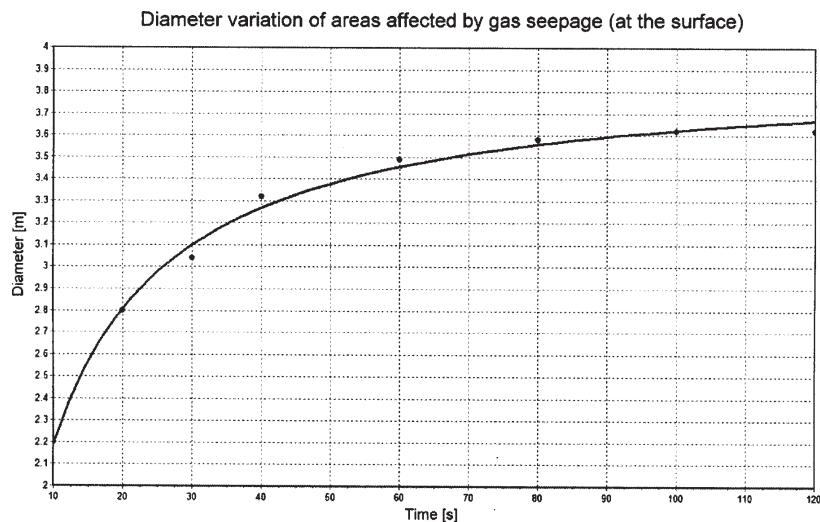


Fig. 4. Diameter variation of areas affected by gas seepage during transitory period

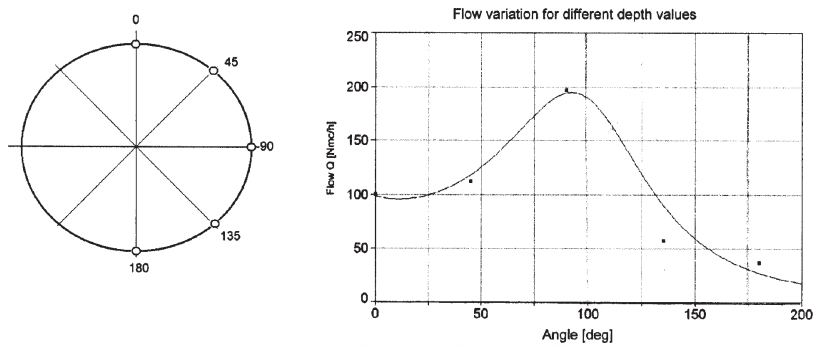


Fig. 5. Flow rates of the gas seeped through soil and surfaced specific for various positions of the defect. Below are pictures representing the distribution of gas flow rates specific for two positions of the defect.

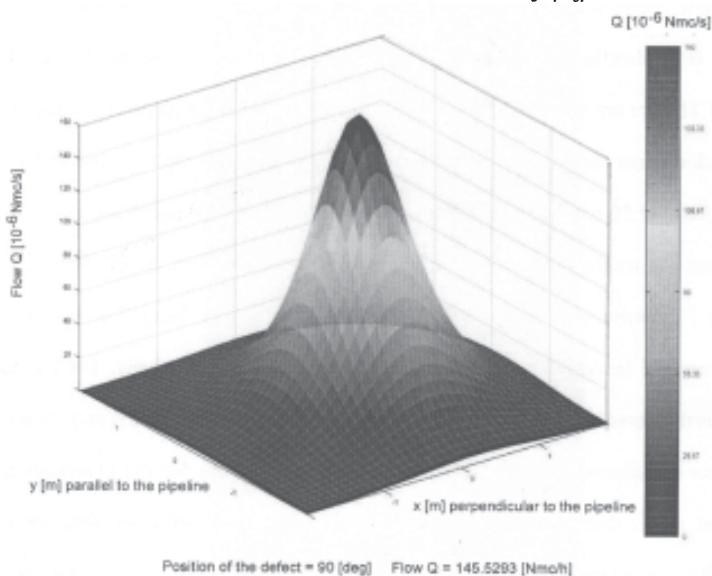


Fig. 6. Distribution of gas flow at soil surface for a defect positioned at 90 °

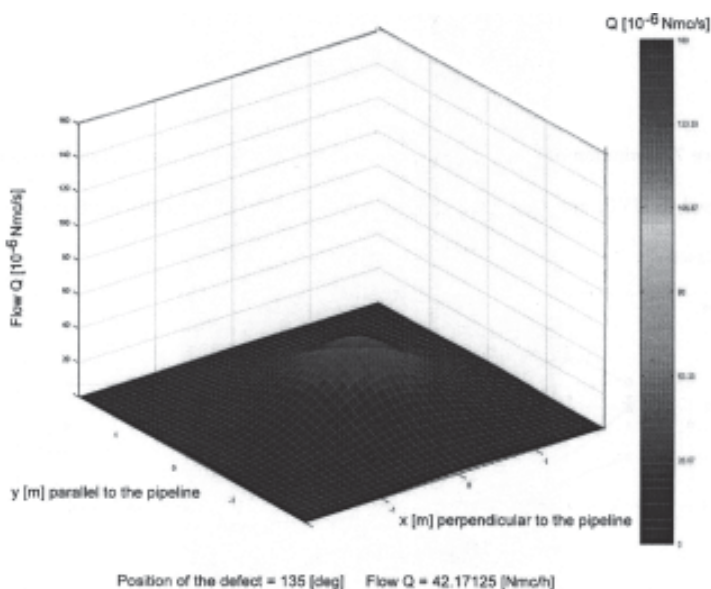


Fig. 7. Distribution of gas flow at soil surface for a defect positioned at 135 °

The mathematical expression of this curve is shown in equation (11).

$$D = \frac{1}{a+b/x} [m] \quad (11)$$

where the parameters are:  $a = 0.25599142$ ,  $b = 1.9991142$

*Analysis of the influence played by the defect position along the pipeline on the leak flow through the soil*

Since the model used was a 3D one, it was possible to perform an analysis of the influence of the position of the defect along the pipeline on the seeped through the ground and eventually surfaced gas flow. For this purpose several simulations have been conducted considering different positions of the defect. Figure 5 depicts a section of the

pipeline along which various angular positions of the defect are delineated. The conducted simulations were adapted for the following positions: 0°, 45°, 90°, 135° and 180°. The curve representing the change of the flow rates of seeped gas considering the position of the defect is:

$$Q = 1/(a + bx + cx^2 + dx^3) \quad (12)$$

where  $x$  represents the angular position of the defect, expressed in degrees, and the coefficients of the function are:  $a = 0.01069444$ ,  $b = 6.1856791e-05$ ,  $c = -3.1072933e-06$ ,  $d = 2.0008606e-08$ .

Below are pictures representing the distribution of gas flow rates specific for two positions of the effect.



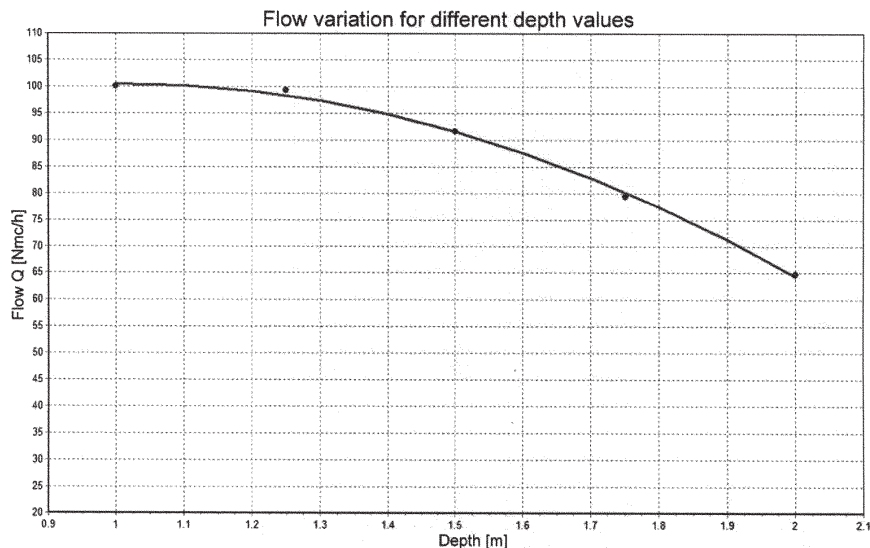


Fig. 8. Influence of the depth on the flow rate of gas seeped into soil and surfaced

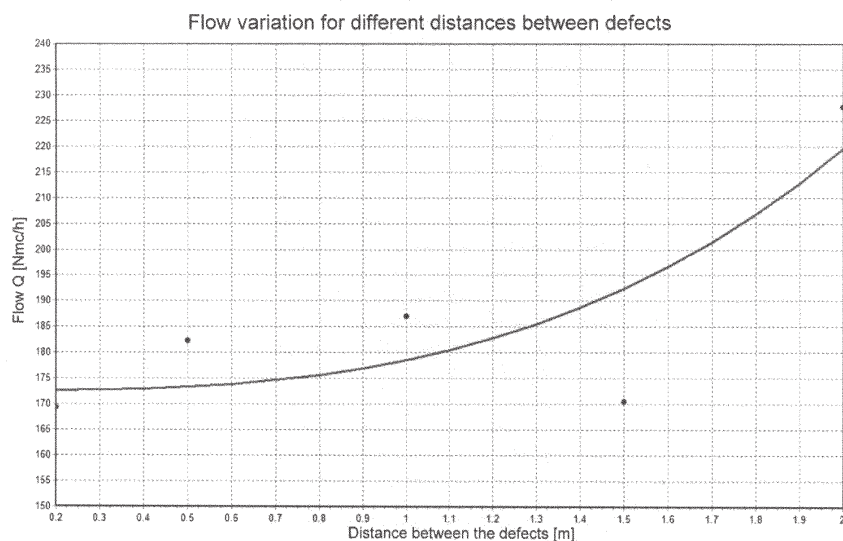


Fig. 9. Variation of seeped gas flow into soil and its surfacing depending on the distance between the defects

*The influence of burial depth of the pipeline on the flow rate of gas which has reached the surface ground*

For this particular analysis it has been considered a defect positioned above the pipeline at an angle of  $0^\circ$ , while the burial depth of the pipeline has been established to vary from 1 to 2m deep. The results obtained are outlined in figure 8, which features a graph that shows the variation in flow for different depths values.

The benchmark flow value considered for this analysis has been set at a depth of 1m (100%) and all the other flow depths have been consequently expressed as a percentage relating to this benchmark. It has been observed that the flow rate of gas seeped through the soil and the one which reached the surface decreases with the depth of burial of the pipeline.

The function that describes this behaviour is

$$Q = a + bx + cx^2 \quad [\text{Nm}^3/\text{h}] \quad (13)$$

where  $x$  stands for the depth of burial of the pipe calculated in meters and the constants are:  $a = 63.129686$ ,  $b = 74.068114$ ,  $c = -36.740571$

It is noted (fig. 14) that in the case of a 2m burial depth of the pipeline, the seeped gas flow through the soil which reached the surface ground decreases to 65 % of the flow rate specific for a 1m burial depth of the pipeline.

*Analysis of the influence played by the distance between the defects on the flow rate calculated at the surface of the ground*

For situations where several corrosion defects may occur along the pipeline, an analysis has been performed considering a pipeline on which 3 identical failures were defined, located in the same angular position of  $0^\circ$ , at different distances. The seeped gas flows move into the soil due to pressure gradients. The position and distance between the defects alters the seeped gas flows into the soil and the ones that reach the surface. Figure 9 is a graphical representation of this case.

To simulate this situation it was considered a pipeline with multiple identical defects located on the generator of the pipeline, at various distances.

Analyzing the results of this simulation reveals that the flow rate measured at the ground surface tends to increase with distance, as represented in figure 9.

The function representing this trend is

$$Q = a + bx^3 \quad [\text{Nm}^3/\text{h}] \quad (14)$$

where  $x$  represents the distance calculated in meters between the defects and the constants are:  $a = 172.67003$ ,  $b = 5.8510425$ .

One of the images depicting the flow distribution on the surface of the ground specific for these tests is graphically

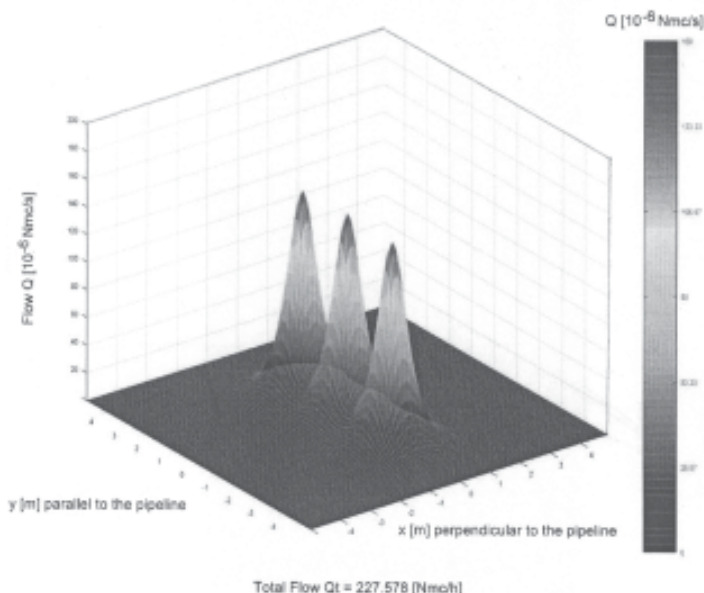


Fig. 10. Flow distribution at the surface specific for a distance of 2 m between defects

presented in figure 10. The distance between defects alters gas seepage affected area. When the distance between defects is less than 1.5m the effects cumulate resulting in a central area with high levels of gas leak. If the distance increases, reaching for example 2 or even more meters, the gas leaks through the defects become individualized.

### Conclusions

An unsteady 3D model has been designed in order to study the gas leak through defects of buried pipelines and to highlight thus the factors on which the gas leaks depend.

The model has outlined that the highest rate of diffused gas flow in the atmosphere is specific for a defect located at  $90^\circ$  from the vertical axis of the pipeline, while the lowest flow rate is reached in the case of a defect located at  $180^\circ$ , which is practically under the pipeline.

The flow rates of leaks reaching the surface decrease with the depth of the pipeline.

### References

1. MINESCU, M., PANĂ, I., Safety Evaluation of the Pipelines Systems for Petroleum Products, Applied Mechanics and Materials, Trans Tech Publications Inc., 371, 2013, p. 782
2. ALBULESCU, M., EPARU, C., MEDREA, L., METEA, V., Calculation of Natural Gas Losses through Buried Distribution Pipes Faults,

Petroleum-Gas University of Ploiesti Bulletin, Technical Series, LXIII, 3, 2011, p. 77

3. STAN, AL.D., POPOVICIU, E., Asupra canalizării gazelor către imobile, Studies and Research in Applied Mechanics, Publishing House of the Academy of the Socialist Republic of Romania, Tome 40, No. 5, 1981, p. 683

4. STAN, AL.D., Scurgerile de gaze prin defectele conductelor, CCPGM Mediaș, 1982

5. OROVEANU, T., STAN, AL.D., Scurgerea gazelor prin defectele conductelor de transport subterane, Studies and Research in Applied Mechanics, Publishing House of the Romanian Academy, Tome 52, No. 6, 1993, p. 503

6. OROVEANU, T., TRIFAN, C., ALBULESCU, M., An Improvement of the Methods for Studying the Gas Flow through Porous Media, Petroleum-Gas Institute of Ploiesti Bulletin, Technical Series, XLIV, 1, 1992, p. 23

7. STAN, AL.D., MINESCU, FL., Scurgerile de gaze prin mediile poroase superficiale, Studies and Research in Applied Mechanics, Publishing House of the Academy of the Socialist Republic of Romania, Tome 42, No. 6, 1983, p. 547

8. POPOVICIU, S., Studiul diminuării pierderilor de gaze din rețelele de distribuție și al reducerii efectelor nocive ale infiltrării acestor gaze prin sol, PhD Thesis, Ploiești, 1982

9. STAN, AL.D., Pierderile de gaze prin defectele conductelor în condiții dinamice, Colloquium on Fluid Mechanics, Mediaș, 1985

Manuscript received: 21.05.2014